Dimerization-induced spin-charge coupling in one-dimensional Mott insulators revealed by femtosecond reflection spectroscopy of Rb-tetracyanoquinodimethane salts

H. Uemura,[1] N. Maeshima,[2,3] K. Yonemitsu,[4,5] and H. Okamoto[1,6]

[1]*Department of Advanced Materials Science, University of Tokyo, Chiba 277-8561, Japan*

[2]*Institute of Materials Science, University of Tsukuba, Ibaraki 305-8577, Japan*

[3]*Center for Computational Sciences, University of Tsukuba, Ibaraki 305-8577, Japan*

[4]*Institute for Molecular Science, Aichi 444-8585, Japan*

[5]*Department of Functional Molecular Science, Graduate University for Advanced Studies, Aichi 444-8585, Japan*

[6]*CREST, Japan Science and Technology Agency (JST), Tokyo 102-0075, Japan*

(Received 6 February 2012; published 14 March 2012)

Effects of lattice dimerizations on charge dynamics in one-dimensional (1D) half-filled Mott insulators were studied using an organic compound, Rb-tetracyanoquinodimethane (TCNQ). First, we investigated the presence of the dimeric molecular displacements by the measurements of polarized Raman spectra and the time evolutions of photoinduced reflectivity changes. The results indicate that Rb-TCNQ shows a spin-Peierls-like structural phase transition and molecular dimerization occurs below 220 K. Second, we performed femtosecond reflection spectroscopy from visible to infrared regions down to 0.1 eV on Rb-TCNQ in both the low-temperature phase with dimerization and the high-temperature phase without dimerization. The results revealed that the molecular dimerization causes splitting of midgap absorption due to photocarriers. Theoretical calculations by the density-matrix renormalization group method reveal that low- and high-energy midgap absorptions are due to pure charge excitation and spin-charge-coupled excitation, respectively, of polarons stabilized by the electron-lattice interaction. This indicates that dimerization breaks the spin-charge separation characteristic of 1D Mott insulators with large electron correlation.

DOI: 10.1103/PhysRevB.85.125112 PACS number(s): 78.40.Me, 71.10.Fd, 71.38.−k, 78.47.jg

I. INTRODUCTION

In one-dimensional (1D) electron systems with large on-site Coulomb repulsion (U), spin and charge degrees of freedom are decoupled with each other.[1,2] Such a feature called spin-charge separation is a key concept in understanding charge dynamics in 1D Mott insulators (MIs). In a previous experiment, the spin-charge separation in 1D MIs was demonstrated by angle-resolved photoelectron spectroscopy of a 1D cuprate, $SrCuO_2$.[3] In that study, holon and spinon dispersions were detected separately. More recently, femtosecond (fs) pump-probe (PP) reflection spectroscopy of a 1D MI of an organic compound, bis(ethylenedithio)tetrathiafulvalene- difluorotetracyanoquinodimethane (ET-F_2TCNQ), revealed that a Drude-type metallic state was generated not only by a large photocarrier doping [0.1 photon (ph)/ET] but also by a small one (0.003 ph/ET).[4,5] In contrast, spin-charge coupling in two-dimensional (2D) and three-dimensional (3D) MIs disturbs free motion of charge carriers, causing midgap absorptions instead of a simple Drude response. Midgap absorptions were in fact generated in 2D MIs of cuprates, La_2CuO_4 and Nd_2CuO_4, by photocarrier doping[6,7] as well as chemical carrier doping.[8,9] Therefore, the Drude response observed irrespective of photocarrier density in ET-F_2TCNQ is clear evidence for the spin-charge separation in 1D MIs.

Generally, in half-filled 1D systems, electron-lattice (e-l) interaction plays an important role in their charge dynamics. In another 1D MI of a Ni-Br chain compound, $[Ni(chxn)_2Br]Br_2$ (chxn: cyclohexanediamine), a metallic state was also photogenerated, when the excitation photon density is large (>0.1 ph/Ni).[10] In the case of a small excitation density (<0.04 ph/Ni), a metallic state did not appear and instead a midgap absorption appeared suggesting that polaronic states were formed due to the e-l interaction. In cases where U is much larger than the transfer energy t, a half-filled 1D MI can be regarded as an antiferromagnetic spin ($S = 1/2$) chain [Fig. 1(a)]. Such a system sometimes shows lattice dimerization at low temperatures [Fig. 1(b)], which is caused by magnetic energy gain owing to the formation of a spin singlet in dimers. This structural transition is called the spin-Peierls transition, which originates from spin-lattice (s-l) interaction.[11] In fact, in most of the half-filled 1D MIs, the lattice is dimerized owing to e-l or s-l interactions at low temperatures.[12,13]

When the lattice is dimerized, charge dynamics in 1D MIs characterized by the spin-charge separation are expected to be modified. However, such effects of lattice dimerization have not yet been clarified. An effective method for investigating charge dynamics is to measure reflectivity changes in the infrared (IR) region induced by photocarriers. In this paper, we report photoinduced reflectivity spectra of a half-filled 1D MI, Rb-tetracyanoquinodimethane (Rb-TCNQ).[14,15]

Alkali (M = Na, K, Rb)-TCNQ is an ion radical salt in which an electron is transferred from M to TCNQ. The molecular structure of TCNQ is shown in Fig. 1(c). In M-TCNQ, $TCNQ^-$ molecules stack one dimensionally [Fig. 1(d)], forming half-filled π-electron bands. Because of large U (∼1.5 eV) on TCNQ overcoming the electron transfer energy t between the neighboring TCNQ molecules,[16,17] M-TCNQ becomes a 1D MI. Various kinds of M-TCNQ salts commonly show the decrease of spin susceptibility below transition temperatures T_c.[18] These transitions are considered as spin-Peierls transitions. In fact, in Na-TCNQ, K-TCNQ, and

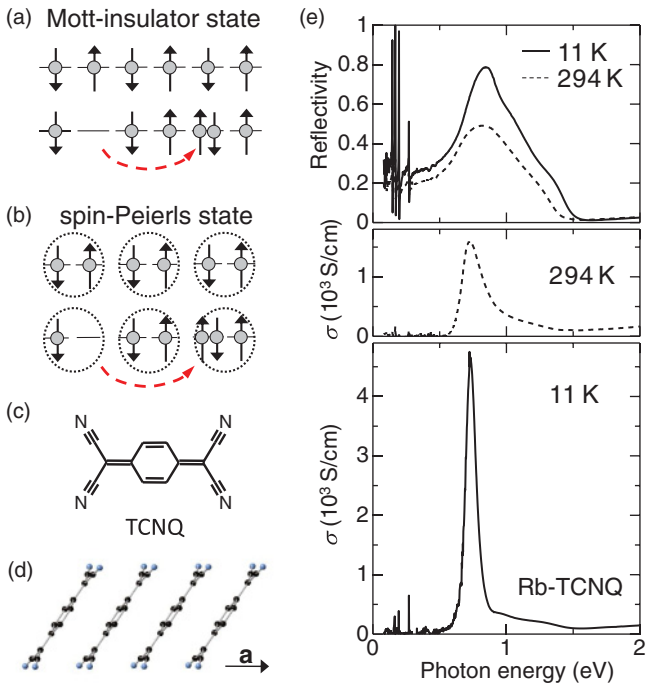

FIG. 1. (Color online) Schematic views of the (a) Mott-insulator state and (b) spin-Peierls state. The broken arrows show photoexcitations. (c) Molecular structure of TCNQ. (d) Stacking structure of $TCNQ^{-}$ in Rb-TCNQ. (e) Reflectivity (R) and optical conductivity (σ) spectra of Rb-TCNQ at 294 and 11 K.

Rb-TCNQ(I), it has been confirmed from the x-ray diffraction studies that the structural transitions from regularly stacked phase to dimerized phase occur at T_c.[19] Rb-TCNQ has three polymorphisms. Rb-TCNQ(I) has monoclinic structure.[20] In the present study, we focus on another polymorphism of Rb-TCNQ with triclinic structure,[14,15] which is called Rb-TCNQ(II). This compound also shows the decrease of spin susceptibility below $T_c = 220$ K similarly to the other alkali-TCNQ salts. Therefore, this magnetic transition had been considered a spin-Peierls transition.[18,21] However, the dimeric structure below T_c has not been clarified by x-ray-diffraction studies probably because the dimeric displacement is very small.[15]

On the basis of these backgrounds, in the present study, we first examined dimerizations in the low-temperature phase of Rb-TCNQ(II) by the measurements of Raman-scattering spectra and photoinduced coherent molecular oscillations. The results revealed that photoresponses showed specific features to those of spin-Peierls systems with lattice dimerizations. This indicates that in Rb-TCNQ(II), 1D molecular stacks are dimerized below 220 K and this structural transition corresponds to the magnetic transition temperature T_c. After that, we studied the main subject; that is, the effect of dimerizations on photocarrier dynamics in Rb-TCNQ(II). When the lattice is dimerized, a Drude-like reflection band observed in the regular lattice in the high-temperature phase was split into two bands. Comparison of the spectral shapes of the two bands with those obtained by theoretical calculations based on the density-matrix renormalization-group (DMRG) method[22,23] revealed that both bands are due to polaronic carriers. The lower-energy band originates from a pure charge excitation and the higher-energy one originates from spin-charge-coupled excitation. We show that the spin-charge separation is broken by the lattice dimerization.

II. EXPERIMENT

Single crystals of Rb-TCNQ were grown by the diffusion method.[14] Rb-TCNQ has three polymorphisms. The material studied here is type II with triclinic structure. We hereafter call it Rb-TCNQ.

To obtain linear optical spectra, polarized reflectivity spectra were measured by using a specially designed spectrometer and Fourier transform infrared spectrometer, both of which were equipped with an optical microscope. In the Raman-scattering measurements, we used a He-Ne laser with 1.96 eV as the incident light and adopted a backscattering configuration. The scattered light was monochromized by a double-grating monochromator and detected by a charge-coupled device detector.

To measure photoinduced reflectivity spectra and photoinduced coherent oscillation, we used fs PP spectroscopy with time resolutions of 180 and 30 fs, respectively, which were based on a Ti:AlO_3 regenerative amplifier [$\sim$800 nm (1.55 eV), pulse width of 130 fs, and repetition rate of 1 kHz]. The output of the amplifier was divided into two beams. In 180 fs measurement, one was used for a pump light, and the other for excitation of an optical parametric amplifier (OPA), from which the probe light (0.1–2.5 eV) was obtained. In 30 fs measurement, the divided two beams were used for excitation of two noncollinear OPAs, from which pump pulses and probe pulses were obtained. The temporal widths of the pump and probe pulses were 16 and 23 fs, respectively, and the time resolution was about 28 fs, which was enough to detect the dynamics of molecular displacements. Delay time t_d of the probe pulse relative to the pump pulse was controlled by changing the path length of the pump pulse. The excitation photon density within the penetration depth of pump light l_p was evaluated from the formula $x_{\mathrm{ph}} = I_p(1 - R_p)(1 - 1/e)/l_p$. Here, I_p and R_p are the photon density per unit area and the reflection loss of the pump light, respectively.

III. RESULTS AND DISCUSSION

A. Linear optical spectra

Figure 1(e) shows the reflectivity (R) spectra of Rb-TCNQ at 11 and 294 K with the electric field (**E**) of lights parallel to ($\|$) **a** and the optical conductivity (σ) spectra obtained from the R spectra by the Kramers-Kronig transformation. At 294 K, σ shows an asymmetric single peak at $\sim$0.7 eV. This band corresponds to the Mott gap transition. σ spectra in half-filled 1D MIs were theoretically studied by applying the DMRG method to the extended Hubbard model including U, t, and the intersite Coulomb repulsion V.[24] The theoretical result indicated an asymmetric single peak, which was in agreement with the observation result. In the spectrum at 11 K, the higher-energy shoulder structure ranging from 0.9 to 1.4 eV was split off from the main peak. The previous experimental[25] and theoretical[17] studies on a similar dimerized MI, K-TCNQ, suggest that this shoulder structure of Rb-TCNQ would also

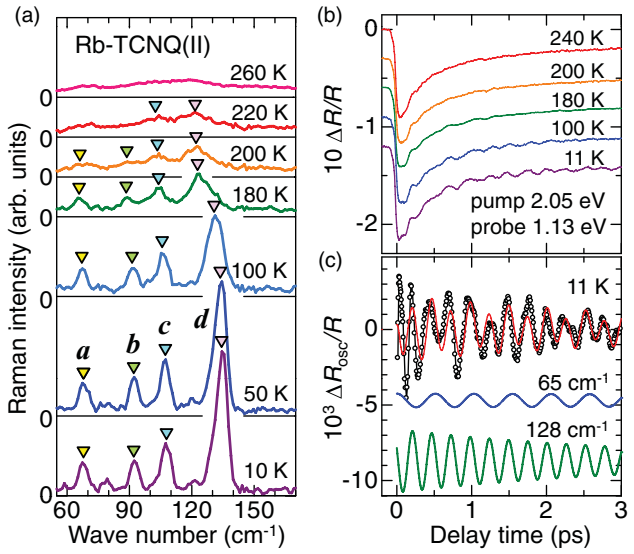

FIG. 2. (Color online) (a) Temperature dependence of the polarized Raman spectra. The electric field of the incident light $\boldsymbol{E}_i$ and that of the scattering light $\boldsymbol{E}_s$ were polarized parallel and perpendicular to **a**, respectively. (b) Temperature dependence of the photoinduced reflectivity changes $\Delta R/R$ at 1.13 eV. (c) The oscillatory component (open circles) at 11 K and the simulation [the thin red (dark gray) line]. Each oscillatory component with 65 and 128 cm^{-1} was also shown in the lower part (thick lines).

originate from lattice dimerization. In the next section, the presence of molecular dimerizations is discussed in more detail.

B. Molecular dimerizations in Rb-TCNQ

As for the lattice dimerizations, Raman-scattering spectra give important information. It is because in this type of 1D molecular compounds, symmetry breaking of the lattice should give rise to activations of lattice modes in Raman spectra. Therefore, we measured the temperature dependence of the Raman spectra in Rb-TCNQ. Figure 2(a) shows temperature dependence of polarized Raman-scattering spectra from 55 to 170 cm^{-1}. The electric field of the incident light $\mathbf{E}_i$ was parallel to ($\parallel$) the stacking axis **a** and that of the scattering light $\mathbf{E}_s$ was perpendicular ($\perp$) to **a**. Four bands **a**, **b**, **c**, and **d** with the frequencies of $\sim$65, $\sim$90, $\sim$105, and $\sim$125 cm^{-1} were activated below T_c, respectively. With decrease of temperature, the intensities of those bands are enhanced and the frequencies are slightly increased.

The activations of the Raman bands suggest that in Rb-TCNQ, the lattice symmetry is broken below T_c by the dimerization. In the polarization configuration with $\mathbf{E}_i \parallel \mathbf{a}$ and $\mathbf{E}_s \perp \mathbf{a}$, possible candidates of the Raman modes activated in the low-temperature phase are shear-type modes.[26] Two degrees of freedom exist in shear-type molecular displacements so that two kinds of shear-type modes are possible, while four modes were observed in the experiments. Therefore, other molecular degrees of freedom such as molecular bending might be related to the molecular dimerizations in addition to the shear-type displacements.

For the configuration with $\mathbf{E}_i \parallel \mathbf{a}$ and $\mathbf{E}_s \parallel \mathbf{a}$, the band **d** at $\sim$125 cm^{-1} was also activated below T_c, but no other bands were detected in the measured region. The mode with $\sim$125 cm^{-1} has the same mode (a shear-type mode or a bending mode) as observed for $\mathbf{E}_s \perp \mathbf{a}$. If dimeric molecular displacements along the stacking axis **a** exist, the corresponding Raman band will be detected in this configuration. It may appear in the lower frequency region below 50 cm^{-1}.

We can also obtain valuable information about molecular dimerizations from transient photoresponses. When the alkali-TCNQ salts such as K-TCNQ and Na-TCNQ in the spin-Peierls phase are irradiated with a fs laser pulse, the dimeric molecular displacements are released through the destabilization of the spin-Peierls phase.[26,27] This phenomenon is called a photoinduced melting of the spin-Peierls phase. In these phenomena, it was revealed that coherent oscillations corresponding to the releases of the dimeric molecular displacements were observed on the photoinduced changes $\Delta R/R$ of the reflectivity R. This is because the dimeric molecular displacements modulate the energy of the Mott gap transition. If the dimerizations occur in Rb-TCNQ below $T_c =$ 220 K, similar coherent oscillations should be detected by an irradiation of a fs laser pulse. On the other hand, if the lattice is not dimerized, there is no reason for such coherent oscillations to appear.

Figure 2(b) shows the temperature dependence of the time characteristics of $\Delta R/R$. The pump (2.05 eV) and the probe (1.13 eV) lights were polarized parallel to the stacking axis **a**. The excitation photon density was 0.02 ph/TCNQ. The coherent oscillations were observed on $\Delta R/R$ below $T_c = 220$ K and increased their amplitudes with decrease of temperature. Therefore, it is natural to consider that these oscillations are related to the spin-Peierls transition; that is, to the dimeric molecular displacements. By subtracting the background time profile from $\Delta R/R$, we obtained oscillatory components $\Delta R_{\text{osc}}/R$. The time profile of $\Delta R_{\text{osc}}/R$ at 11 K was shown by open circles in Fig. 2(c). This oscillatory component was almost reproduced by the sum of two damped oscillators with the frequencies of 65 and 128 cm^{-1} shown by a thin red (dark gray) line in the same figure, which was expressed as

$$\frac{\Delta R_{\text{osc}}}{R} = \sum_{i=1,2} A_i \cos(\omega_i t + \phi_i) \exp\left(-\frac{t}{\tau_i}\right). \qquad (1)$$

The initial phase of the 128 cm^{-1} mode is $\sim$66°. Therefore, the main component of this oscillation is of a sine type and is attributable to an impulsive stimulated Raman scattering. On the other hand, the initial phase of the 65 cm^{-1} mode is equal to zero, suggesting that the oscillation is of a cosine type. Therefore, this oscillation is attributable to the displacive excitation of coherent oscillation.[28] The open squares in Fig. 3 show the temperature dependence of the oscillation amplitudes of the 65 cm^{-1} mode. The amplitude increases with decrease of temperature. Taking account of the fact that similar coherent oscillations induced by a fs laser pulse were observed in the spin-Peierls phases of K-TCNQ and Na-TCNQ, it is natural to consider that the observed oscillation (the 65 cm^{-1} mode) in Rb-TCNQ is due to the photoinduced melting of the spin-Peierls dimerizations. In fact, the amplitude of the 65 cm^{-1} mode increases below 220 K (Fig. 3), indicating a strong correlation to the temperature dependence of the magnetic susceptibility.[18]

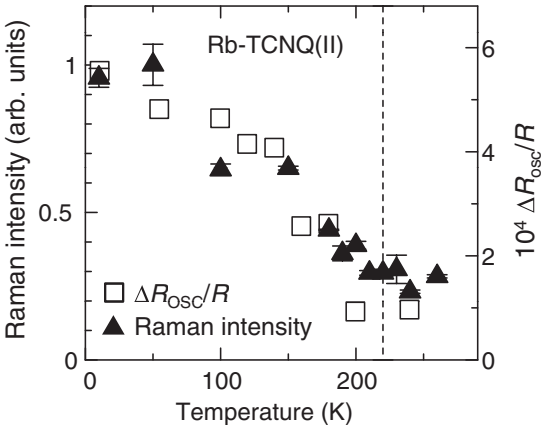

FIG. 3. Temperature dependence of the amplitude of the coherent oscillation with 65 cm^{-1} (squares) and the integrated intensity of the Raman band **a** (triangles) measured from the background level.

The frequencies, 65 and 128 cm^{-1}, of two coherent oscillations correspond well to the frequencies of the Raman bands **a** and **d**, respectively. In Fig. 3, we show the temperature dependence of the integrated intensity of the Raman band **a** by solid triangles, which is in good agreement with that of the amplitude of the coherent oscillation $\Delta R_{osc}/R$ of the Raman band **a** with 65 cm^{-1} (open squares). From these results, we can conclude that the spin-Peierls transition with molecular dimerizations occurs in Rb-TCNQ and the corresponding lattice mode becomes Raman active below $T_c = 220$ K and that the dimeric molecular displacements are released by the photoirradiation as observed in K-TCNQ and Na-TCNQ.[26,27]

C. Transient reflectivity changes

In order to investigate the effect of lattice dimerization on charge dynamics in more detail, we measured the photoinduced transient reflectivity spectra in a wide frequency region down to about 0.1 eV in both the high-temperature and low-temperature phases of Rb-TCNQ. The spectra of photoinduced reflectivity changes (ΔR) at 11 K are shown in Fig. 4(a) together with those at 294 K, previously reported.[21] The electric fields of the pump and probe lights were $\|\mathbf{a}$. The excitation photon density was 0.09 ph/TCNQ.

At 294 K in the high-temperature phase, R decreased above 0.4 eV and increased below 0.4 eV, indicating a transfer of the spectrum weight from the gap transition to the IR region owing to photocarrier doping. ΔR below 0.4 eV monotonically increased with decreasing energy, showing photogeneration of a conducting state. At 11 K in the low-temperature phase, R also showed a spectral weight transfer from the gap transition to the IR region. ΔR showed a plus-minus structure above 0.5 eV, which reflects the redshift of the gap transition due to the photoinduced melting of the spin-Peierls dimerization, as previously discussed.[26,27] In the IR region, ΔR showed a characteristic spectral shape different from that at 294 K; the spectrum was split into a high-energy band that peaked at ~0.25 eV, labeled as **A**, and a low-energy band below 0.2 eV, labeled as **B**. Such a change in ΔR from 294 to 11 K is attributable to lattice dimerization. The signals in the IR region decayed within a few picoseconds at both temperatures, showing rapid photocarrier recombination.

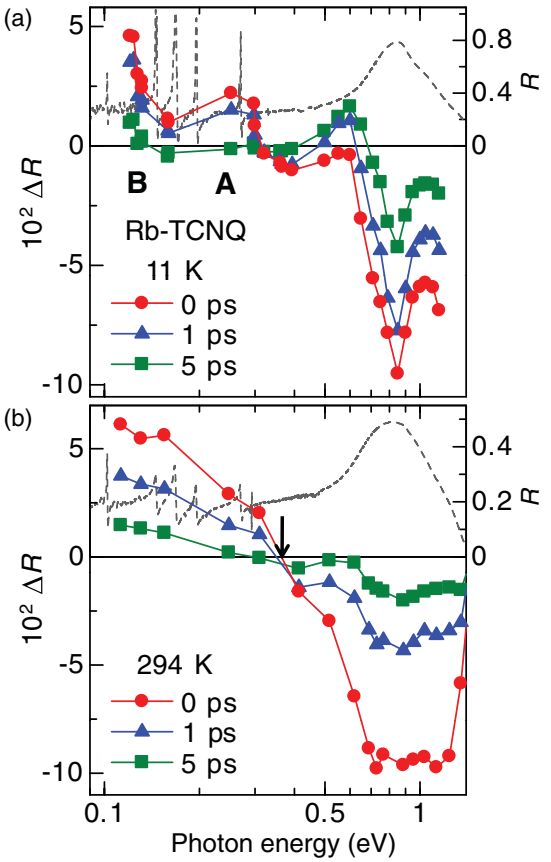

FIG. 4. (Color online) Spectra of photoinduced reflectivity change (ΔR) at (a) 11 and (b) 294 K in Rb-TCNQ. Polarizations of both pump and probe pulses are parallel to the stacking axis **a**. The broken lines show the original R spectra. An arrow in (b) indicates the crossing energy E_c at which $\Delta R = 0$.

D. Dimerization-induced spin-charge coupling

To investigate the origin of bands **A** and **B**, we theoretically calculated the absorption spectra by applying the DMRG method to the extended Peierls-Hubbard model, described by the following Hamiltonian:[17]

$$H = -\sum_{l=0,\sigma}^{N-2} t_0(1+u_l)(c^+_{l+1,\sigma}c_{l,\sigma} + c^+_{l,\sigma}c_{l+1,\sigma}) + U\sum_{l=0}^{N-1} n_{l,\uparrow}n_{l,\downarrow} + V\sum_{l=0}^{N-2} n_l n_{l+1} + \frac{K_\alpha}{2}\sum_{l=0}^{N-2} u_l^2 + \Gamma\sum_{l=0}^{N-2} u_l. \quad (2)$$

Here, $t_0 = (t_1 + t_2)/2$ is the average of intradimer transfer energy t_1 and interdimer transfer energy t_2, and u_l is the lattice distortion. K_α is the elastic constant and Γ is the parameter introduced to keep the chain length the same as that of the original configuration. At half filling, the lattice distortion is

fixed to $u_l = (-1)^l\delta$, where $\delta = (t_1 - t_2)/(t_1 + t_2)$ is the distortion parameter.

First, to determine the basic parameters U, V, t_0, and δ, we referred to a previous study on K-TCNQ,[17] which showed spin-Peierls transition at 395 K.[18,19] In that study, δ at 294 K in the low-temperature phase was evaluated to be 0.46 by calculation of transfer energies based on the extended Hückel method.[29] U and t_0 were determined to be 1.45 and 0.29 eV, respectively, which could reproduce well the σ spectrum for the gap transition using the dynamical-DMRG method. U is inherent to the molecule, so the same U value can be adopted in Rb-TCNQ. In Rb-TCNQ, δ is unknown, since the dimerization in the low-temperature phase is too small to be determined by x-ray-diffraction measurements,[15] as detailed in Sec. III B. The intensity of σ for the gap transition integrated from 0.5 to 1.6 eV at 11 K in Rb-TCNQ was 1.4 times that at 294 K in K-TCNQ,[21] suggesting that t_0 is larger in Rb-TCNQ at 11 K. The lower spin-Peierls transition temperature and the larger t_0 in Rb-TCNQ as compared to K-TCNQ suggest that the e-l (or s-l) interaction is weaker in Rb-TCNQ and therefore $\delta < 0.46$. Considering this, we examined the four cases of $\delta = 0.1$, 0.2, 0.3, and 0.4 in the system with 50 sites. K_α was determined to attain a given δ value in a stable lattice configuration, and the other parameters, V and t_0, were determined to reproduce the experimental σ spectrum. Figure 5(a) shows the calculated σ spectra for $\delta = 0.1$–0.4 (broken lines), in which the broadening parameter ε was taken into account. The spectrum for $\delta = 0.2$ reproduced well the experimental spectrum, particularly the shoulder structure at higher energy, which emerges due to the lattice dimerization as mentioned above. The parameters used were $V = 0.578$, $t_0 = 0.428$, $K_\alpha = 3.05$, and $\varepsilon = 0.039$ eV. For $\delta = 0.1$, V was decreased to reproduce the energy of the main peak, resulting in the calculated spectrum being quite different from the experimental one owing to a small excitonic effect. For $\delta = 0.3$ and 0.4, V was rather enhanced to reproduce the peak energy of the experimental spectrum; however, the shoulder structures could not be reproduced well.

Next, we investigated the change in the σ spectrum by the introduction of an additional carrier (an electron) in the half-filled system. First, we determined the one-electron ground state by the DMRG method under lattice relaxation; then, we calculated σ by a previously reported procedure,[17] in which the broadening parameter ε was set to be 0.051 eV. In the upper panel of Fig. 5(b), the calculated σ for $\delta = 0.2$ in the IR region is shown, which reproduced well both bands **A** and **B** in the experimental ΔR spectrum at $t_d = 0$ ps.

To clarify the nature of these two bands, we calculated the spatial profiles of charge density $\langle n\rangle$ and spin density $\langle S\rangle$ in the ground state and the two optically excited states corresponding to bands **A** and **B**. The calculation method used has been reported elsewhere.[17] Figure 6(a) shows the profiles of $\langle n\rangle$ and $\langle S\rangle$ in the ground state [i] and changes in the profiles by transitions corresponding to bands **A** and **B**. In the ground state [i], the distributions of the charge and spin density are quite similar and range over ~15 sites around the center. This indicates that the additional electron is stabilized as a polaron. The molecular displacements are also continuously changed around the center (not shown), as reported for a polaron in K-TCNQ.[17] For the lower-energy transition **B**, the changes in charge density ($\Delta\langle n\rangle$) and spin density ($\Delta\langle S\rangle$) are equal

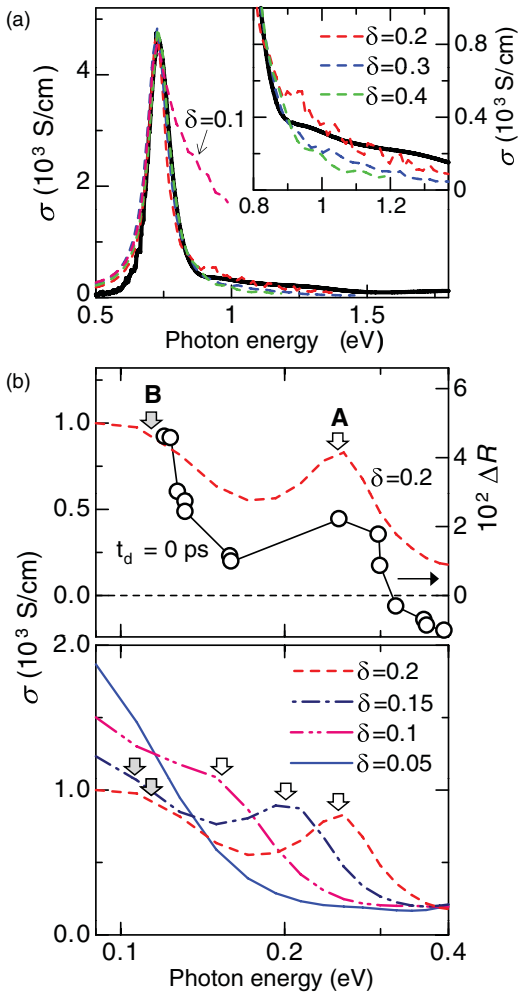

FIG. 5. (Color online) (a) Experimental σ spectrum at 11 K (solid line) and calculated σ spectra for $\delta = 0.1$–0.4 (broken lines). (b) Upper panel: ΔR spectrum (open circles) in the IR region at $t_d = 0$ ps and the calculated σ spectrum (broken line) for the one-electron doped state with a parameter set of $\delta = 0.2$ ($V = 0.578$ eV, $t_0 = 0.428$ eV, $K_\alpha = 3.05$ used in (a), and $\varepsilon = 0.051$ eV). Lower panel: δ dependence of σ spectra for the one-electron doped state with $V = 0.578$ eV, $t_0 = 0.428$ eV, and $\varepsilon = 0.051$ eV. δ was changed by adjusting K_α.

to each other, having minima of envelopes at the center and maxima on the right- and left-hand sides. This indicates that band **B** corresponds to a simple charge excitation of the polaron [Fig. 6(b) [i] → [ii]]. In this figure, only the excitation to the right-hand side is shown, although the actual excitation is the linear combination of two excitations to the right- and left-hand sides. For the higher-energy transition **A**, the charge density decreases at the center and increases on the right- and left-hand sides, similar to the lower-energy transition **B**. On the other hand, the spin density increases at the center and decreases on the right- and left-hand sides. This shows that the spin and charge degrees of freedom are excited in different regions. This excitation is illustrated in Fig. 6(b) [i] → [iii], in which up-spin triplet excitation occurs at the two central sites, while the total spin moment remains unchanged, since a down spin is generated in the dimer on the right-hand side [Fig. 6(b) [iii]]. Thus, a charge excitation by light causes additional changes in spin configurations. This indicates that band **A** corresponds

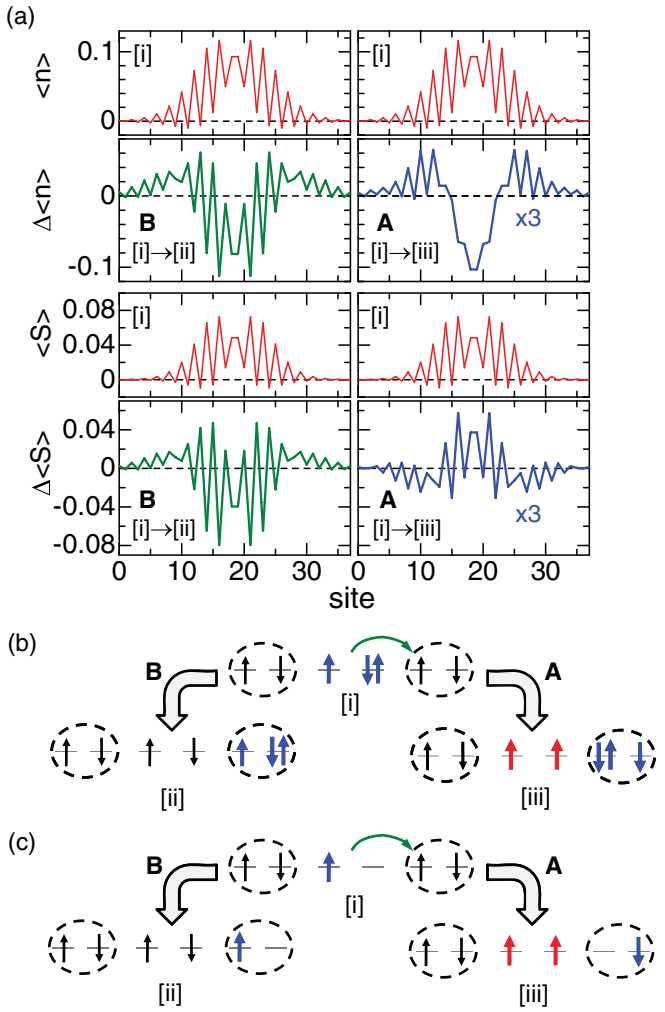

FIG. 6. (Color online) (a) Spatial distributions of charge density $\langle n \rangle$ and spin density $\langle S \rangle$ in the one-electron doped state of a dimerized MI [i] and their changes $\Delta\langle n \rangle$ and $\Delta\langle S \rangle$ caused by transitions **A** and **B**. Schematic views of the (b) electron polaron state and (c) hole polaron state and their optical transitions; [i]: polaron ground state, [i]→[ii]: simple charge excitation, and [i]→[iii]: spin-charge-coupled excitation.

to a spin-charge-coupled excitation. In the present system, electron-hole symmetry exists, so a hole polaron should exhibit the similar optical transitions to those of an electron polaron [Fig. 6(c)]. Since the spin-charge separation stands in regular 1D MIs, such a coupling is attributable to lattice dimerization.

The splitting of **A** and **B** (∼0.15 eV) is a crude measure for the triplet excitation energy, which increases with lattice dimerization. When δ is decreased from 0.2 to 0.05 by changing only K_α and keeping the other parameters (U, V, and t_0) fixed, the splitting between **A** and **B**, indicated by the arrows in Fig. 5(b), reduces and the spectral weight shifts to the lower-energy side as shown in the lower panel of Fig. 5(b). For $\delta = 0.05$, the splitting cannot be identified. These behaviors are consistent with our interpretation.

Taking the simplified picture shown in Figs. 6(b) and 6(c) into account, even in a regular 1D MI, similar spin-charge coupling is expected to occur if a carrier is localized as a polaron owing to the *e-l* interaction. In the high-temperature phase of Rb-TCNQ, a Drude-like response was observed by photoirradiation [Fig. 4(b)] as mentioned above. Strictly, however, the ΔR spectrum cannot be explained by a simple Drude response.[21] In a Drude model, the crossing energy (E_c) at $\Delta R = 0$ is a rough measure for the plasma frequency, and therefore, E_c should decrease with decreasing photocarrier density over time.[4] In contrast, in Rb-TCNQ, E_c (∼0.35 eV) remains almost unchanged with time, as indicated by the arrow in Fig. 4(b). This suggests that photocarriers would be affected by polaron effects and that the charge-spin coupling would be included in the ΔR responses.

IV. SUMMARY

From the temperature dependences of polarized Raman spectra and time characteristics of photoinduced reflectivity changes, we confirmed that molecular dimerizations occur in the low-temperature phase of Rb-TCNQ. We have also measured the transient reflectivity spectra in the low-temperature phase and found that a photocarrier produced two midgap absorption bands. By comparing their spectral features with the theoretical calculation results, the lower-energy midgap absorption band was assigned to a pure charge excitation and the higher-energy one was assigned to a spin-charge-coupled excitation. It was indicated that lattice dimerization breaks the spin-charge separation in a one-dimensional Mott insulator.

ACKNOWLEDGMENTS

This work was supported in part by a Grant-in-Aid by MEXT (No. 20110005) and JSPS (No. 21·6182).

[1] J. Sölyom, Adv. Phys. **28**, 201 (1979).
[2] M. Ogata and H. Shiba, Phys. Rev. B **41**, 2326 (1990).
[3] C. Kim, A. Y. Matsuura, Z.-X. Shen, N. Motoyama, H. Eisaki, S. Uchida, T. Tohyama, and S. Maekawa, Phys. Rev. Lett. **77**, 4054 (1996).
[4] H. Okamoto, H. Matsuzaki, T. Wakabayashi, Y. Takahashi, and T. Hasegawa, Phys. Rev. Lett. **98**, 037401 (2007).
[5] S. Wall, D. Brida, S. R. Clark, H. P. Ehrke, D. Jaksch, A. Ardavan, S. Bonora, H. Uemura, Y. Takahashi, T. Hasegawa, H. Okamoto, G. Cerullo, and A. Cavalleri, Nat. Phys. **7**, 114 (2011).
[6] H. Okamoto, T. Miyagoe, K. Kobayashi, H. Uemura, H. Nishioka, H. Matsuzaki, A. Sawa, and Y. Tokura, Phys. Rev. B **82**, 060513(R) (2010).
[7] H. Okamoto, T. Miyagoe, K. Kobayashi, H. Uemura, H. Nishioka, H. Matsuzaki, A. Sawa, and Y. Tokura, Phys. Rev. B **83**, 125102 (2011).
[8] S. Uchida, T. Ido, H. Takagi, T. Arima, Y. Tokura, and S. Tajima, Phys. Rev. B **43**, 7942 (1991).
[9] Y. Onose, Y. Taguchi, K. Ishizaka, and Y. Tokura, Phys. Rev. B **69**, 024504 (2004).

[10]S. Iwai, M. Ono, A. Maeda, H. Matsuzaki, H. Kishida, H. Okamoto, and Y. Tokura, Phys. Rev. Lett. **91**, 057401 (2003).
[11]For a review, see J. W. Bray, L. V. Interrante, I. S. Jacobs, and J. C. Bonner, in *Extended Linear Chain Compounds*, edited by J. S. Miller (Plenum Press, New York, 1983), Vol. 3, p. 353.
[12]J. B. Torrance, in *Low-Dimensional Conductors and Superconductors*, edited by D. Jerome and L. G. Caron, NATO Advanced Study Institutes, Series B, Vol. 155 (Plenum Press, New York, 1987).
[13]K. Yonemitsu and M. Imada, Phys. Rev. B **54**, 2410 (1996).
[14]H. Kobayashi, Bull. Chem. Soc. Jpn. **54**, 3669 (1981).
[15]T. M. McQueen, D. M. Ho, C. J. Cahua, R. J. Cava, R. A. Pascal Jr., and Z. G. Soos, Chem. Phys. Lett. **475**, 44 (2009).
[16]K. Yakushi, T. Kusaka, and H. Kuroda, Chem. Phys. Lett. **68**, 139 (1979).
[17]N. Maeshima and K. Yonemitsu, J. Phys. Soc. Jpn. **77**, 074713 (2008).
[18]J. G. Vegter and J. Kommandeur, Mol. Cryst. Liq. Cryst. **30**, 11 (1975).
[19]H. Terauchi, Phys. Rev. B **17**, 2446 (1978).
[20]A. Hoekstra, T. Spoelder, and A. Vos, Acta Crystallogr. Sect. B: Struct. Crystallogr. Cryst. Chem. **28**, 14 (1972).
[21]H. Uemura, H. Matsuzaki, Y. Takahashi, T. Hasegawa, and H. Okamoto, J. Phys. Soc. Jpn. **77**, 113714 (2008).
[22]S. R. White, Phys. Rev. Lett. **69**, 2863 (1992).
[23]E. Jeckelmann, Phys. Rev. B **66**, 045114 (2002).
[24]E. Jeckelmann, Phys. Rev. B **67**, 075106 (2003).
[25]H. Okamoto, Y. Tokura, and T. Koda, Phys. Rev. B **36**, 3858 (1987).
[26]K. Ikegami, K. Ono, J. Togo, T. Wakabayashi, Y. Ishige, H. Matsuzaki, H. Kishida, and H. Okamoto, Phys. Rev. B **76**, 085106 (2007).
[27]H. Okamoto, K. Ikegami, T. Wakabayashi, Y. Ishige, J. Togo, H. Kishida, and H. Matsuzaki, Phys. Rev. Lett. **96**, 037405 (2006).
[28]H. J. Zeiger, J. Vidal, T. K. Cheng, E. P. Ippen, G. Dresselhaus, and M. S. Dresselhaus, Phys. Rev. B **45**, 768 (1992).
[29]T. Mori, A. Kobayashi, Y. Sasaki, H. Kobayashi, G. Saito, and H. Inokuchi, Bull. Chem. Soc. Jpn. **57**, 627 (1984).